High-precision U-Pb zircon igneous crystallization and detrital zircon maximum depositional ages from the Toodoggone region, north-central British Columbia

Luke Ootes and Corey Wall

BRITISH COLUMBIA
Ministry of
Energy, Mines and
Low Carbon Innovation

Open File 2024-06

Ministry of Energy, Mines and Low Carbon Innovation
Responsible Mining and Competitiveness Division
British Columbia Geological Survey

Recommended citation:2024. High-precision U-Pb zircon igneous crystallization and detrital zircon maximum depositional ages from the Toodoggone region, north-central British Columbia. British Columbia Ministry of Energy, Mines and Low Carbon Innovation, British Columbia Geological Survey Open File 2024-06, 10p.

Front cover:
Black Lake intrusive suite granodiorite outcrop sampled for U-Pb zircon geochronolgy. Omineca Resource Road, view to the north. **Photo by Luke Ootes.**

Back cover:
Toodoggone Formation (Hazelton Group) basal conglomerate, stratigraphically above the unconformity with subjacent Takla Group rocks, containing subrounded and subangular cobbles and boulders in a sandstone matrix, which was sampled for U-Pb detrital zircon geochronology. View to the north. **Photo by Luke Ootes**.

BRITISH COLUMBIA

Ministry of
Energy, Mines and
Low Carbon Innovation

High-precision U-Pb zircon igneous crystallization and detrital zircon maximum depositional ages from the Toodoggone region, north-central British Columbia

Luke Ootes
Corey Wall

Ministry of Energy, Mines and Low Carbon Innovation
British Columbia Geological Survey
Open File 2024-06

High-precision U-Pb zircon igneous crystallization and detrital zircon maximum depositional ages from the Toodoggone region, north-central British Columbia

Luke Ootes[1a] and Corey Wall[2]

[1] British Columbia Geological Survey, Ministry of Energy, Mines and Low Carbon Innovation, Victoria, BC, V8W 9N3
[2] Pacific Centre for Isotopic and Geochemical Research, Department of Earth, Ocean and Atmospheric Sciences, Vancouver, BC Canada V6T 1Z4
[a] corresponding author: Luke.Ootes@gov.bc.ca

Recommended citation: Ootes, L. and Wall, C., 2024. High-precision U-Pb zircon igneous crystallization and detrital zircon maximum depositional ages from the Toodoggone region, north-central British Columbia. British Columbia Ministry of Energy, Mines and Low Carbon Innovation, British Columbia Geological Survey Open File 2024-06, 10p.

Abstract
In geological environments that rapidly evolved, high-precision geochronologic techniques such as chemical abrasion isotope dilution thermal ionization mass spectrometry (CA-TIMS) may be needed to resolve temporal uncertainties from less precise laser ablation inductively coupled plasma mass-spectrometry (LA-ICP-MS). The Toodoggone region of eastern Stikine terrane hosts Late Triassic to Early Jurassic porphyry Cu-Au and epithermal Au-Ag deposits. Mineralization is in the Asitka, Takla, and Hazelton groups and allied granitic intrusions. In north-central Toodoggone region, the areally extensive but undivided Black Lake intrusive suite is spatially related to numerous epithermal mineralized zones. Two new U-Pb zircon ages from the Black Lake intrusive suite, determined by high-precision CA-TIMS indicate that early granodiorite crystallized at 202.87 ± 0.03 Ma (n=6/6; MSWD=1.2) and slightly younger quartz monzonite at 200.02 ± 0.03 Ma (n=6/6; MSWD = 0.8). The results are similar to previous ages for Kemess porphyry Cu-Au mineralization in southern Toodoggone region. Detrital zircons analyzed by LA-ICP-MS from conglomerates at the base of the Toodoggone Formation (Hazelton Group) indicate that they were sourced from the Asitka Group (ca. 313 Ma) and immediately underlying Takla Group (225 and 207 Ma) and yield a maximum likely age (MLA) of 196 ± 3.8 Ma. Analysis of detrital zircons from an interflow sandstone higher in section indicate derivation from coeval volcanic rocks (ca. 200 Ma); six of the youngest grains from this sample were measured by the CA-TIMS method, yielding a precise maximum depositional age (MDA) of 194.96 ± 0.04 Ma (n=3/6; MSWD=1.5). The results are interpreted to indicate that the Toodoggone Formation post-dates crystallization of the main phases of the Black Lake intrusive suite, and that epithermal mineralization in the Toodoggone Formation cannot be linked in time to these intrusive rocks.

Keywords: Toodoggone Formation, Black Lake intrusive suite, U-Pb zircon, CA-TIMS, detrital zircon geochronology

1. Introduction

Laser ablation inductively coupled plasma mass-spectrometry (LA-ICP-MS) has become a standard technique for U-Pb zircon geochronology (e.g., Ootes et al., 2022). Although extremely useful, this technique may not provide the precision required to establish the depositional, volcanological, intrusive, structural, hydrothermal, and mineralizing history of areas that evolved rapidly. Instead, high-precision methods, such as chemical abrasion isotope dilution thermal ionization mass spectrometry (CA-TIMS), may be needed to separate discrete events that followed in rapid succession.

Stikine terrane (or Stikinia, Late Triassic to Jurassic) of the Cordilleran orogen (Fig. 1) hosts many porphyry Cu-Au, epithermal Au-Ag±Cu, and volcanogenic massive sulphide deposits (e.g., Nelson et al., 2013). In eastern Stikinia (Fig. 2), the Toodoggone region hosts a past-producing porphyry deposit (Kemess) and several epithermal Au deposits (e.g., Baker, Lawyers, Shasta). Work by Duuring et al. (2009) and Bouzari et al. (2019) indicated that the time span for mineralization in the Toodoggone region is only about 20 million years (~205 to 185 Ma), and that Kemess porphyry mineralization (ca. 200 Ma) in the south is slightly older than epithermal mineralization (<194 Ma) in the north. However, the dates presented on maps in Diakow (2001) and Diakow et al. (1993, 2006) and in a compilation by Duuring et al. (2009) are of uncertain vintage and reliability. Furthermore, recent LA-ICP-MS U-Pb zircon igneous crystallization age determinations (Bouzari et al., 2019) are difficult to assess because interpretations typically rely on weighted means of >20 single zircon U-Pb analyses, with individual results that can span more than 20 million years of uncertainty. The weighted mean ages may be accurate, but they are not precise enough to confidently resolve the short time frames of Late Triassic to Early Jurassic magmatic activity in the Toodoggone region. The CA-TIMS method provides single zircon results that are typically concordant, with analytical uncertainties <<1 Ma to <0.1 Ma (ie., 10x to >100x more precise than individual LA-ICP-MS results).

Supracrustal rocks in the Toodoggone region include three unconformity bounded sequences: the Asitka Group (Carboniferous-Permian); the Takla Group (Upper Triassic);

and the Hazelton Group (Lower Jurassic). In the north-central part of the Toodoggone area (Fig. 2), the Black Lake intrusive suite (or Duncan pluton, e.g., Bouzari et al., 2019) cuts Asitka and Takla group rocks. These rocks are unconformably overlain by the Toodoggone Formation, a unit in the lower part of the Hazelton Group. Although areally extensive and a multiphase body (Diakow et al., 1993, 2006) the Black Lake intrusion has not been subdivided into subunits. The northern extent of the suite appears to coincide with the hinge zone of a regional anticlinorium, and volcanic-hosted epithermal mineralization appears to be preserved along the axial trace of the anticlinorium (Ootes, 2023). This relationship led Ootes (2023) to hypothesize that deformation and this epithermal mineralization may have been synchronous with intrusion. In this paper, we apply the CA-TIMS U-Pb zircon technique, presenting new high-precision dates from two Black Lake samples. We also present new LA-ICP-MS U-Pb detrital zircon ages from a conglomerate at the base of the Toodoggone Formation and an inter-volcanic lithic sandstone higher in the section. To establish a precise maximum depositional age of this sandstone (see e.g., Harriott et al., 2019), six of the youngest zircons from the lithic sandstone that were analyzed by LA-MS-U-Pb were plucked from grain mounts and reanalyzed by CA-TIMS.

The two Black Lake phases crystallized at 202.87 ± 0.03 Ma and, nearly 3 million years later, at 200.02 ± 0.03. The maximum depositional age determined from our CA-TIMS analyses of the youngest zircon grains in the lithic sandstone (194.96 ± 0.04 Ma) is several million years younger than the intrusive suite and porphyry mineralization in the region, falsifying the hypothesis that intrusion, deformation, and epithermal mineralization were synchronous.

2. Eastern Stikinia

2.1. Stratigraphic framework

Eastern Stikinia is underlain by the Asitka Group (Carboniferous-Permian; equivalent to the Stikine assemblage in western Stikinia), the Takla Group (Upper Triassic; equivalent to the Stuhini and Lewes River groups in western and northern Stikinia), the Hazelton Group (Lower Jurassic), and plutons (Late Triassic to Early Jurassic, Fig. 2). The eastern exposures of Stikinia are in fault contact with Quesnel and Cache Creek terranes; to the west, Stikinia is overlain by the Bowser Lake and Sustut groups (Late Jurassic to Cretaceous; Figs. 1,2; e.g., Lord, 1948; Diakow, 2001; Diakow et al., 1993, 2006; Evenchick et al., 2007).

In the Toodoggone area (Fig. 2), the Asitka Group consists of predominantly fossiliferous carbonate rocks that are

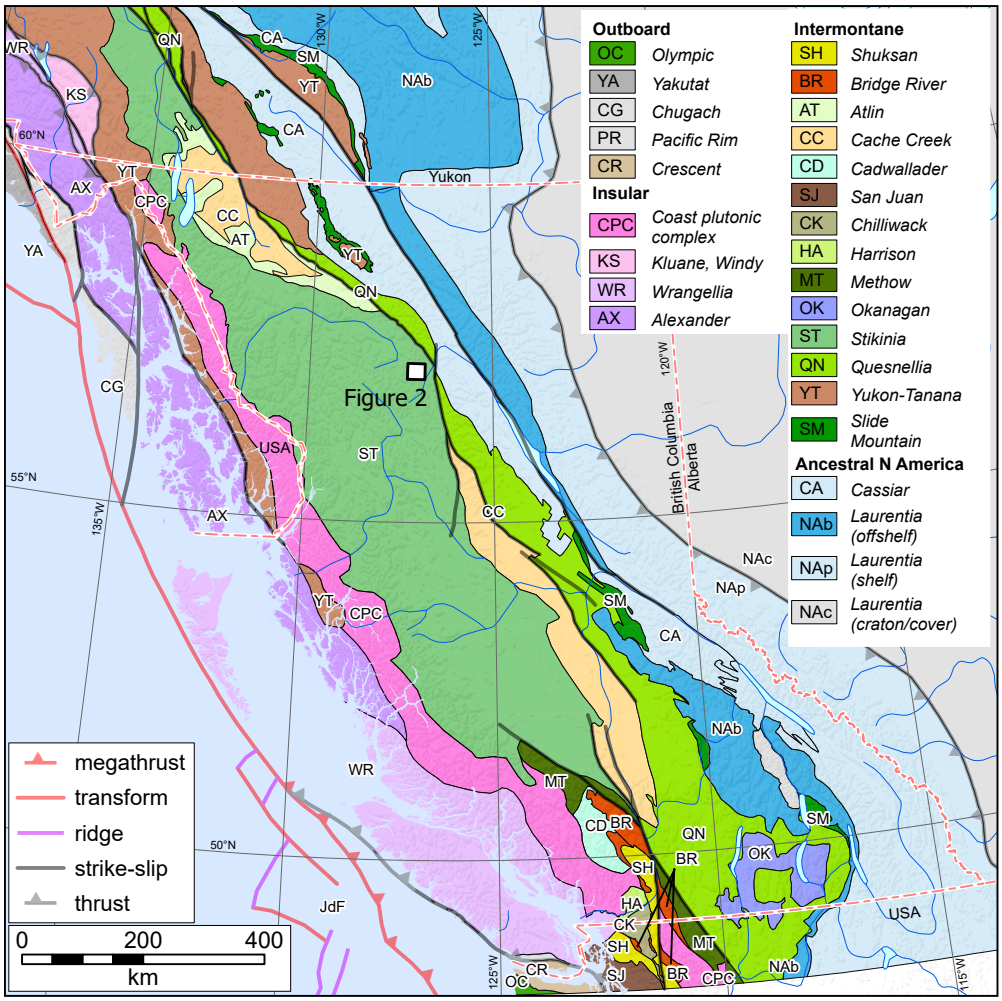

Fig. 1. Location of the north-central Toodoggone region, eastern Stikine terrane. Terranes modified from Colpron (2020).

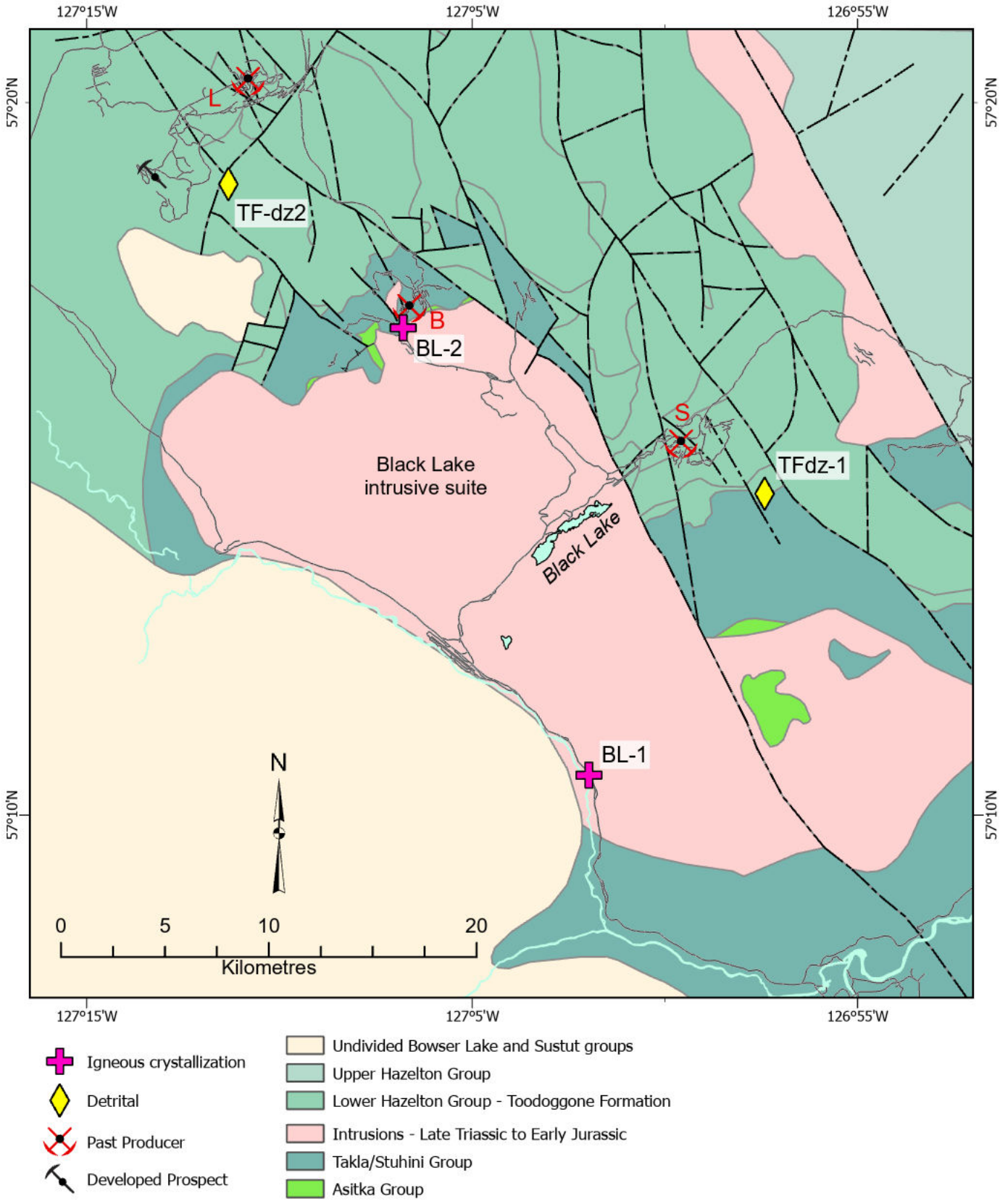

Fig. 2. Geology of the north-central Toodoggone region. For simplicity, the Toodoggone Formation has not been subdivided into its members. Simplified after Diakow et al. (1993, 2006). B-Baker mine; L-Lawyers mine; S-Shasta mine.

unconformably overlain by siltstones and sandstones and volcanic rocks of the Takla Group (Late Triassic). These are in turn unconformably overlain by the Toodoggone Formation of the Hazelton Group (Early Jurassic); the base is a locally preserved unit of polymitic conglomerate and interbedded sandstone, a few m thick, that is overlain by massive intermediate volcanic flows and tuffaceous rocks (Diakow et al., 1993; 2006).

In southern Toodoggone, the Asitka and Takla groups are intruded by several Early Jurassic plutons (Diakow, 2001; Duuring et al., 2009). In north-central Toodoggone, a relatively large body of quartz monzonite is referred to as the Black Lake intrusive suite (Fig. 2; Early Jurassic; Diakow et al., 1993; 2006; Duncan pluton in Bouzari et al., 2019). This intrusive body is spatially related to the Baker and Shasta epithermal deposits, but the internal intrusive phases remain undivided (Fig. 2; Diakow et al., 2006). Bouzari et al. (2019) provided a Re-Os molybdenite date from the Baker mine (ca. 194 Ma), and LA-ICP-MS U-Pb zircon dates from the Blake Lake intrusive suite (Duncan pluton), supporting Early Jurassic crystallization ages (ca. 200 Ma).

3. Analytical Methods

3.1. LA-ICP-MS

All samples were processed at the University of British Columbia, Pacific Centre for Isotopic and Geochemical Research (UBC-PCIGR). Abundant (>200) zircon crystals, 20-150 microns long and with a mixed morphology were separated from hand samples by conventional density and magnetic methods. The entire picked zircon separate was placed in a muffle furnace at 900°C for 60 hours in quartz beakers to anneal minor radiation damage; annealing enhances cathodoluminescence (CL) emission (Nasdala et al., 2002), promotes more reproducible inter-element fractionation during laser ablation inductively coupled plasma mass spectrometry (LA-ICPMS; Allen and Campbell, 2012), and prepares the crystals for subsequent chemical abrasion (Mattinson, 2005). Following annealing, individual grains from all samples were hand-picked based on morphology, clarity, and the absence of inclusions and mounted in epoxy for imaging.

Mounted grains of zircon were imaged for internal structure at the Electron Microbeam/X-Ray Diffraction Facility (EMXDF) at University of British Columbia using a Philips Xl-30 scanning electron microscope (SEM). Zircon grains were imaged using a Robinson cathodoluminescence (CL) detector, using a Bruker Quanta 200 energy-dispersion X-ray microanalysis system with XFlash 6010 SDD detector at a voltage of 15 kV.

Trace element concentrations were determined in zircon by laser ablation inductively coupled plasma mass spectrometry (LA-ICP-MS) at PCIGR using a Resonetics (now ASI) RESOlution M-50-LR Class I laser ablation system coupled to an Agilent 7700x quadrupole ICP-MS. Ablations were carried out with a 193nm excimer laser, using a beam energy of 100 mJ and a pit diameter of 34 μm, with a pulse rate of 5 Hz for 30 seconds followed by 20 seconds of gas blank. Spots were chosen based on grain-scale variations observed in CL images and grain size, with typically two analyses per grain. For zircon, measurements were conducted on the masses ^{7}Li, ^{29}Si, ^{31}P, ^{45}Sc, ^{49}Ti, ^{89}Y, ^{91}Zr, ^{93}Nb, ^{139}La, ^{140}Ce, ^{141}Pr, ^{146}Nd, ^{147}Sm, ^{153}Eu, ^{157}Gd, ^{159}Tb, ^{163}Dy, ^{165}Ho, ^{166}Er, ^{169}Tm, ^{172}Yb, ^{175}Lu, ^{177}Hf, ^{188}Ta, ^{202}Hg (as a monitor for Pb), Pb (^{204}Pb, ^{206}Pb, ^{207}Pb, ^{208}Pb), ^{232}Th, and U (^{235}U and ^{238}U); these masses were chosen based on high relative isotopic abundances and the absence of interferences. Sample-standard bracketing was carried out with spot analyses of synthetic glasses NIST 612 and NIST 610 (trace elements) between zircon analyses and the natural zircon reference materials 91500, Plesovice (PL), and Temora2 (TEM) were also analyzed for calibration of U-Pb dates.

Data were reduced using Iolite 4 software running within the Igor Pro environment using the U-Pb geochronology and Trace Elements IS data reduction schemes (Paton et al., 2011). For U-Pb geochronology in zircon, 91500 was used as the calibration standard and reference materials PL and Temora2 were monitored as secondary references for quality assurance and control. For trace elements in zircon, NIST 612 was used as the calibration standard and the average Zr contents (by sample) determined by electron microprobe were employed as an internal standard value for the unknowns. All concentrations are reported in ppm with uncertainties of 2 standard deviation. Analytical results are in Appendix 1.

3.2. CA-TIMS

Three samples were selected for high-precision U-Pb zircon dating by the chemical abrasion isotope dilution thermal ionization mass spectrometry (CA-TIMS; modified after Mattinson, 2005) method at the University of British Columbia, Pacific Centre for Isotopic and Geochemical Research. Dates were obtained from U-Pb analyses of single zircon grains. The youngest grains from LA-ICP-MS results were plucked from their grain mounts and transferred into 3 mL Teflon PFA beakers. The grains were then rinsed in 3.5 M HNO_3 several times before being transferred to 5 μL microcapsules. These microcapsules were placed in a large-capacity Parr vessel, and the zircon was partially dissolved in 120 μL of 29 M HF for 12 h at 200°C. The zircon was returned to 3 mL Teflon PFA beakers, the HF was removed, and the zircon was immersed in 6N HCl, ultrasonically cleaned for an hour, and fluxed on a hotplate at 80C for an hour. The HCl was removed, and the zircon was rinsed twice in ultrapure H_2O before being reloaded into the 300 μL Teflon PFA microcapsules (rinsed and fluxed in 6 M HCl during sonication and washing of the zircon) and spiked with the EARTHTIME mixed ^{233}U–^{235}U–^{205}Pb tracer solution (ET535). Zircon was dissolved in Parr vessels in 120 μL of 29 M HF with a trace of 3.5 M HNO_3 at 220°C for 48 h, dried to fluorides, and re-dissolved in 6 M HCl at 180°C overnight. Solutions were subsequently dried down and redissolved in 60 μL of 3 M HCl to convert to $PbCl_3$-, UO_2Cl_3-, and UCl_6-ions. Uranium and Pb were separated from the zircon matrix using an HCl-based anion-exchange chromatographic procedure (Krogh, 1973). Lead was eluted with 200 μL of 6 M HCl and U with 250 μL of MQ-H_2O into the same beaker and dried with 2 μL of 0.05 N H_3PO_4.

Lead and U were loaded on a single outgassed Re filament in 5 μL of a silica gel/phosphoric acid mixture (Gerstenberger and Haase, 1997), and U and Pb isotopic measurements were made on a Nu Instruments thermal ionization mass spectrometer equipped with an ion-counting Daly detector. Lead isotopes were measured by peak jumping all isotopes on the Daly detector for 100 to 160 cycles. Mass fractionation was

determined using repeat measurements of standard material NBS-981 solution that has equal atom ^{208}Pb and ^{206}Pb and thus measures fractionation directly. It was either 0.16±0.03 % amu^{-1} or 0.18±0.03 % amu^{-1} (1σ) for the analytical sessions reported here. Transitory isobaric interferences due to high-molecular-weight organics, particularly on ^{204}Pb and ^{207}Pb, disappeared within approximately 60 cycles, while ionization efficiency averaged 10^4 cpspg^{-1} of each Pb isotope. Linearity (to cps) and the associated deadtime correction of the Daly detector were monitored by repeated analyses of NBS981. Uranium was analyzed as UO ions in static Faraday mode on 10^{12} Ω resistors for 300 cycles and corrected for isobaric interference of $^{233}U^{18}O^{16}O$ on $^{235}U^{16}O^{16}O$ with and $^{18}O/^{16}O$ ratio of 0.00206. Ionization efficiency averaged 20 mVng^{-1} of each U isotope. Uranium mass fractionation was corrected using the known $^{233}U/^{235}U$ ratio of the tracer solution.

Uranium–Pb dates and uncertainties were calculated using the algorithms of Schmitz and Schoene (2007); calibration of ET535 tracer solution (Condon et al., 2015) of $^{235}U/^{205}Pb$ =100.233, $^{233}U/^{205}Pb$ =0.99506, and $^{205}Pb/^{204}Pb$ =11268; U decay constants recommended by Jaffey et al. (1971); and of $^{238}U/^{235}U$ = 137.818 (Hiess et al., 2012). The $^{206}Pb/^{238}U$ ratios and dates were corrected for initial ^{230}Th disequilibrium using $_{DTh/U}$ = 0.20±0.05 (1σ) and the algorithms of Crowley et al. (2007), resulting in an increase in the $^{206}Pb/^{238}U$ dates of ~0.09 Ma. All common Pb in analyses was attributed to laboratory blank and subtracted based on the measured laboratory Pb isotopic composition and associated uncertainty. Uranium blanks are estimated at 0.013 pg.

4. U-Pb zircon results

Excel files with analytical results from igneous samples are in Appendix 1; results from sedimentary samples are in Appendix 2 (BCGS_OF2024-06.zip).

4.1. Igneous rocks

4.1.1. Black Lake intrusive suite (BL-1; Sample #22lo16-88)

A sample of biotite-hornblende granodiorite, assigned to unit BLqm by Diakow et al. (2006), was collected from bedrock exposures east of Sturdee Valley airstrip, along the Omineca Resource Road (Figs. 2, 3a,b). Zircon grains were analyzed by LA-ICP-MS for U-Pb and trace element systematics. A subset of six individual zircon were selected, removed from the grain mount, and analyzed by TIMS. Results overlap on concordia and yield a weighted mean age of 202.874 ± 0.028 Ma (2σ; MSWD=1.2; Fig. 4a,b; Table 1).

4.1.2. Blake Lake intrusive suite (BL-2; Sample #22lo12-72)

A sample of hornblende-biotite quartz monzonite, assigned to unit BLqm by Diakow et al. (2006), was collected from an exposure on an access road north of the Bakers mine site (Fig. 2, 3c,d). After sample preparation, zircons were analyzed by LA-ICP-MS for U-Pb and trace element systematics. From these analysis, a subset of six individual zircon were removed from their grain mounts and analyzed by TIMS. Results overlap on concordia and yield a weighted mean age of 200.023 ± 0.028 Ma (2σ; MSWD=0.8; Fig. 4c,d; Table 1).

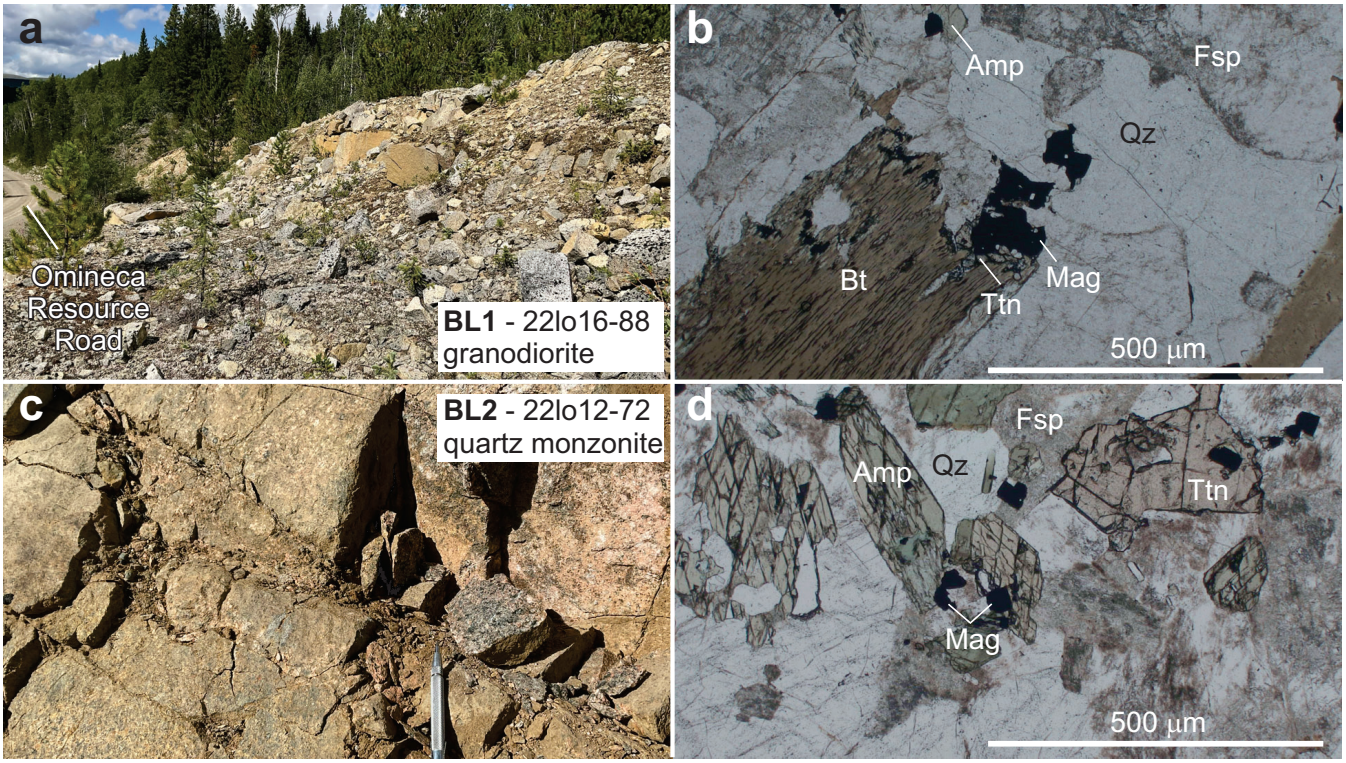

Fig. 3. Black Lake intrusive suite rocks sampled in this study. **a)** Outcrop of granodiorite next to the Omineca Resource Road. View to the north. **b)** Photomicrograph of biotite-hornblende granodiorite. Plane polarized light. **c)** Outcrop of quartz monzonite near Baker mine. **d)** Photomicrograph of hornblende-biotite quartz monzonite. Plane polarized light. Amp-amphibole; Bt-biotite; Fsp-feldspar; Mag-magnetite; Qz-quartz; Ttn-titanite.

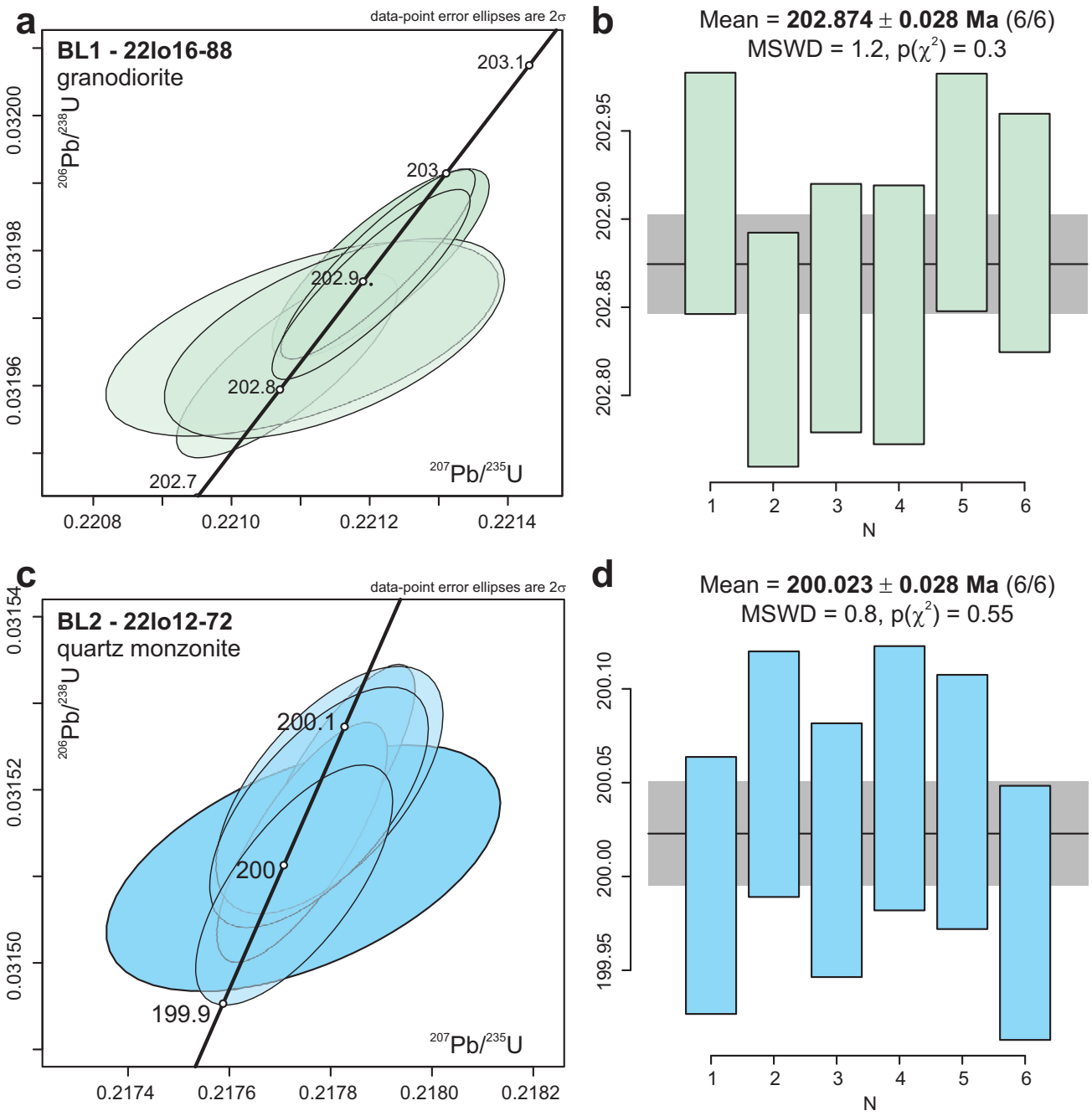

Fig. 4. Results of CA-TIMS U-Pb zircon geochronology for Black Lake intrusive suite samples. **a)** Concordia plot and **b)** weighted mean results from granodiorite BL-1 (sample #22lo16-88). **c)** Concordia plot and **d)** weighted mean results from quartz monzonite BL-2 (sample #22lo12-72). MSWD-mean square of weighted deviation; N-number of zircon on weighted mean plot; p(x^2)-chi square goodness of fit. Sample locations are in Figure 2 and Table 1, and photographs in Figure 2; analytical results are in Appendix 1. Plots generated using IsoplotR (Vermeesch, 2018).

Table 1. Crystallization age determinations.

ID	Sample#	Alias	Lat	Long	Intrusive suite	Age (Ma)	(+/-)	Method
BL-1	22lo16-88	LOO22-16-88	57.176035	-127.032821	Black Lake	202.874	0.028	CA-TIMS
BL-2	22lo12-72	LOO22-12-72	57.280755	-127.113170	Black Lake	200.023	0.028	CA-TIMS

CA-TIMS=chemical abrasion, isotope dilution thermal ionization mass spectrometry

4.2. Sedimentary rocks

4.2.1. Toodoggone Formation (TF-dz1; Sample #22lo14-77)

South of Shasta mine site, the unconformity between Takla Group and overlying Hazelton Group (Toodoggone Formation, Duncan Member, Unit Tc; Diakow et al. 2006) is marked by a basal polymictic cobble to boulder conglomerate (Figs. 2, 5a,b). We sampled the medium-grained sandstone matrix to this conglomerate for detrital zircon analyses. After sample preparation, LA-ICP-MS analyses for U-Pb and trace element systematics, followed by trace element screening of the results, 61 zircon results represent populations between 340 and 300 Ma and 240 to 200 Ma (Figs. 6a,b). Three-component finite unmixing of the detrital zircon data yields calculated populations of 313.4 ± 2.6 Ma (24%), 225.4 ± 2.6 Ma (32%) and 207.0 ± 1.7 Ma (44%) with a maximum likely age (MLA; Vermeesch, 2021) of 196.0 ± 3.8 Ma (Fig. 6b; Table 2). This sample was not selected for additional TIMS analyses.

4.2.2. Toodoggone Formation (TF-dz2; Sample #22gtd027)

A sample of medium- to coarse-grained inter-volcanic lithic sandstone, likely part of the Metsantan Member (Unit TMs) of Diakow et al. (2006), was collected from geotechnical drill core at the Lawyers mine site (Fig. 2, 5c,d). After sample preparation, LA-ICP-MS analyses for U-Pb and trace element systematics, followed by trace element screening of the results (Ootes et al., 2022), 107 zircon results represent a single population centred at about 200 Ma (Fig. 6a). Two-component finite unmixing of the detrital zircon data yields calculated dates of 189.9 ± 2.9 Ma (9.2%) and 196.8 ± 0.8 Ma (91%) with a calculated MLA of 193.5 ± 3.7 Ma (Fig. 6c).

To provide a more accurate and precise maximum deposition age (MDA) we selected six of the youngest zircons were for TIMS. The TIMS analyses yield overlapping concordant results, although one population (n=3) is slightly younger than the other (n=3; Fig. 6e). A weighted mean of the six results yield a MDA of 195.09 ± 0.03 Ma (2σ; MSWD=14), whereas a weighted mean of the youngest three yield a MDA of 194.956 ± 0.043 Ma (2σ; MSWD=1.5; Fig. 6f; Table 2); the MDA of this sample is estimated at 194.96 ± 0.04 Ma.

5. Discussion

5.1. Timing relationships

High-precision U-Pb zircon geochronology from the north-central Toodoggone region further indicates that the Black Lake intrusive suite is a multiphase unit (e.g., Bouzari et al., 2019). The two phases dated in this study include granodiorite from the Omineca Resource Road that crystallized at 202.87 ± 0.03 Ma (BL-1) and quartz monzonite near the Baker mine that crystallized nearly three-million years later, at 200.02 ± 0.03 Ma (BL-2).

Detrital zircons from the sandstone matrix to a basal conglomerate of the Toodoggone Formation (sample TF-dz1) yielded a predominant Triassic population (~76%; Fig. 6a,b). This population is time-equivalent to the Stuhini (Takla) Group volcano-sedimentary and intrusive rocks elsewhere in Stikine terrane (e.g., George et al., 2021; Greig et al., 2021). A less prominent detrital zircon population is Carboniferous (24%; Fig. 6a,b), consistent with derivation from the underlying Asitka Group (Ootes et al., 2022). The lack of abundant ca. 200 Ma zircon in the sample prohibits proximal exposure of the Black Lake intrusive suite during initial deposition of this Toodoggone Formation conglomerate.

Detrital zircons from the inter-volcanic sandstone from the Lawyers mine site area (sample TF-dz2) have a single Late Triassic to Early Jurassic population indicating deposition at or after 194.96 ± 0.04 Ma (Fig. 6c-f). The data collectively support that lower Toodoggone Formation volcanic rocks erupted in a relatively short period of time (potentially as short as 1 million years) and was deposited unconformably on the earlier supracrustal rocks (Asitka and Takla groups) and stratigraphically above the Black Lake intrusive suite (203 to 200 Ma; Figs. 2,4,6).

5.2. Mineralization and deformation

The crystallization ages of the two Black Lake intrusive suite samples presented herein overlap in time with estimates by Duuring et al. (2009) and Diakow et al. (2001) for porphyry Cu-Au mineralization in the Kemess area, although these estimates are largely based on unpublished data and are of uncertain vintage and reliability. The MDA reported for the Toodoggone Formation sample TF-dz1 (194.96 ± 0.04 Ma) further indicates that the epithermal mineralization in the north-central Toodoggone region (e.g., Lawyers, Baker, Shasta; Fig. 2) is younger than Black Lake intrusion, as previously suggested by Clarke and Williams-Jones (1991). This conclusion is supported by field relationships such as at Lawyers where epithermal mineralizing system crosscuts the Toodoggone Formation rocks (Diakow et al., 2006). The results indicate the epithermal mineralization post-dated the predominant intrusive phases of the Black Lake intrusive suite by at least 5 million years and possibly longer (e.g., Clarke and Williams-Jones, 1991).

Based on stratigraphic younging directions, Ootes (2023) described a northward-younging anticlinorium in the region, with Toodoggone Formation volcanic rocks in the northern part younging north and in the southern part younging west, and

Table 2. Detrital maximum deposition age determinations.

ID	Sample#	Alias	Lat	Long	Group	Formation	Member	Age (Ma)	(+/-)	Method
TFdz-1	22lo14-77	LOO22-16-88	57.241968	-126.956850	Hazelton	Toodoggone	Duncan	196	3.8	MLA
TF-dz2	*22gtd027	LOO22-12-72	57.31433	-127.188738	Hazelton	Toodoggone	Metsantan	194.956	0.043	CA-TIMS

*coordinates are drill-collar location

Stratigraphic unit assignment after Diakow et al. (2006).

CA-TIMS=chemical abrasion, isotope dilution thermal ionization mass spectrometry

MLA-Maximum likely age; calculated using Vermeesch (2018, 2021) from Laser ablation inductively coupled plasma mass spectrometry results

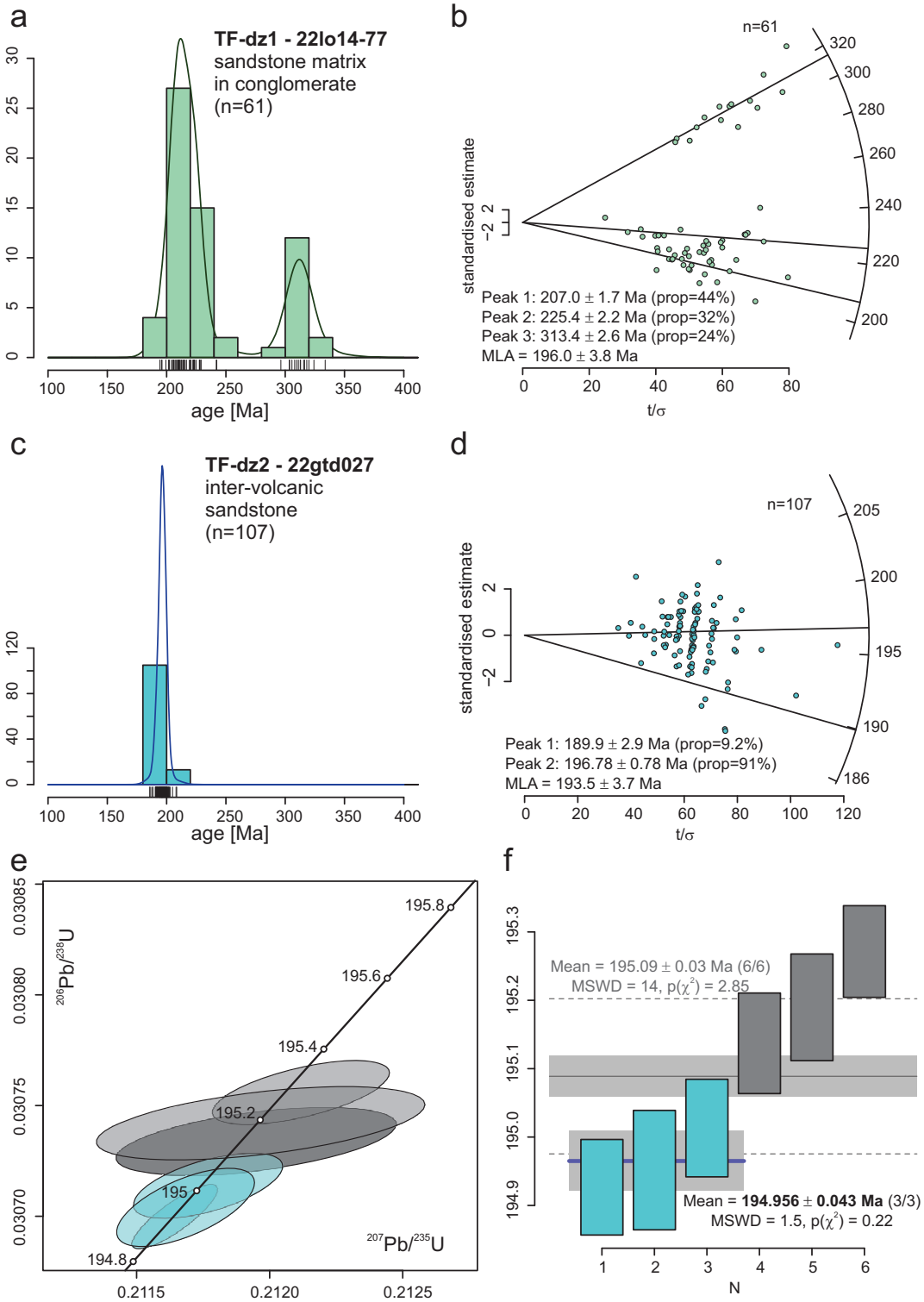

Fig. 6. Results of LA-ICP-MS U-Pb zircon geochronology for TF-dz1 (sample# 22lo14-77). **a)** Kernel density estimate (KDE) diagram and **b)** radial plot with three component finite unmixing results and a maximum likely age (MLA; Vermeesch, 2021). **c)** Results of LA-ICP-MS U-Pb zircon geochronology for TF-dz2 (sample# 22gtd027). Kernel density estimate (KDE) diagram and **d)** radial plot with two component finite unmixing results and a maximum likely age (MLA; Vermeesch, 2021). **e)** Results of CA-TIMS U-Pb zircon geochronology for TF-dz2 (sample# 22gtd027) and **f)** weighted mean plot with two separate results from including six zircon analyzed (grey) and from the three youngest zircon analyzed (blue). MSWD-mean square of weighted deviation; n-number of zircon used in KDE diagrams and radial plots; N-number of zircon on weighted mean plot; p(x^2)-chi square goodness of fit; t/σ- distance from the origin relates to age precision where imprecise measurements plot to the left and more precise age determinations plot to the right (Vermeesch, 2018). Sample locations are in Figure 2 and Table 2, and photographs in Figure 4; analytical results are in Appendix 2. Plots generated using IsoplotR (Vermeesch, 2018, 2021).

with the northern extent of the Black Lake intrusion coinciding with the hinge zone. In addition, Ootes (2023) hypothesized that development of this anticlinorium and epithermal mineralization were synchronous with intrusion of the Black Lake magmas. The high-precision geochronology presented herein falsifies this hypothesis because the Toodoggone Formation rocks that host the epithermal mineralization post-date crystallization of the main phases of Black Lake intrusive suite by at least 5 Ma (Figs. 4,6). The spatial and temporal relationships suggest that the Black Lake intrusion acted as a relatively ridged mechanical anisotropy that controlled folding and preservation of the anticlinorium geometry of the supcracrustal rocks during post-Toodoggone Formation regional shortening.

In short, the data indicate that the epithermal mineralization is not temporally related to the Black Lake intrusive suite. Instead, it may be related to volcanism and sedimentation in the upper part of the Hazelton Group (<195 Ma), which is better preserved in the Toodoggone region northeast of the study area (Fig. 2; Diakow et al., 2006). Thus, epithermal mineralization is younger than major porphyry mineralization in the region (e.g., Kemess deposit, ca. 200 Ma; Duuring et al., 2009).

Acknowledgements

This project benefited from field assistance by Alan West and we thank the PCIGR team (Hai Lin and Taylor Ockerman) for assistance with mineral separation and zircon mounting. TDG Gold Corp. provided access to the Baker and Shasta properties and Thesis Gold provided access to Lawyers and Ranch, as well as accommodations and logistical support at Lawyers camp. Emily Laycock and Rob L'Heureux (Apex Geosciences) provided valuable knowledge about the geology and mineralization at Lawyers and vicinity. Constructive reviews and comments Sean Reagan helped improve the manuscript.

References cited

Allen, C.M., and Campbell, I.H., 2012. Identification and elimination of a matrix-induced systematic error in LA–ICP–MS 206Pb/238U dating of zircon. Chemical Geology 332-333, 157-165. https://doi:10.1016/j.chemgeo.2012.09.038

Bouzari, F., Bissig, T., Hart, C.J.R., and Leal-Mejia, H., 2019. An exploration framework for porphyry to epithermal transitions in the Toodoggone mineral district (94E). Geoscience BC Report 2019-08, 105 p.

Clarke, J.R., and Williams-Jones, A.E., 1991. $^{40}Ar/^{39}Ar$ ages of epithermal alteration and volcanic rocks in the Toodoggone Au-Ag district, north-central British Columbia (94E). In: Geological Fieldwork 1990, British Columbia Ministry of Energy, Mines and Petroleum Resources, British Columbia Geological Survey Paper 1991-1, pp. 207-216.

Colpron, M., 2020. Yukon Terranes - A digital atlas of terranes for the northern Cordillera. Yukon Geological Survey. data.geology.gov.yk.ca/Compilation/2#InfoTab

Condon, D.J., Schoene, B., McLean, N.M., Bowring, S.A., and Parrish, R.R., 2015. Metrology and traceability of U-Pb isotope dilution geochronology (EARTHTIME Tracer Calibration Part I). Geochimica et Cosmochimica Acta, 164, 464-480. https://doi:10.1016/j.gca.2015.05.026

Crowley, J. L., Schoene, B., and Bowring, S. A., 2007. U-Pb dating of zircon in the Bishop Tuff at the millennial scale. Geology, 35, 1123-1126. https://doi.org/10.1130/G24017A.1

Diakow, L.J., 2001. Geology of the southern Toodoggone River and northern McConnell Creek map areas, north-central British Columbia: Parts of NTS 94E/2, 94D/15 and 94D/16. British Columbia Ministry of Energy and Mines, British Columbia Geological Survey Geoscience Map 2001-1, scale 1:50,000.

Diakow, L.J., Panteleyev, A., and Schroeter, T.G., 1993. Geology of the early Jurassic Toodoggone Formation and gold-silver deposits in the Toodoggone River map area, northern British Columbia. British Columbia Ministry of Energy, Mines and Petroleum Resources, British Columbia Geological Survey Bulletin 86, 72 p.

Diakow, L. J., Nixon, G.T., Rhodes, R. and van Bui, P., 2006. Geology of the Central Toodoggone River map area, north-central British Columbia (Parts of NTS 94E/2, 6, 7, 10 and 11). British Columbia Ministry of Energy, Mines and Petroleum Resources, British Columbia Geological Survey Geoscience Map 2006-6, scale 1:50,000.

Duuring, P., Rowins, S.M., McKinley, B.S.M., Dickinson, J.M., Diakow, L.J., Kim, Y.-S., and Creaser, R.A., 2009. Examining potential genetic links between Jurassic porphyry Cu–Au±Mo and epithermal Au±Ag mineralization in the Toodoggone district of North-Central British Columbia, Canada. Mineralium Deposita, 44, 463-496.

Evenchick, C.A., Mustard, P.S., McMechan, M., Ferri, F., Porter, S., Hadlari, T., and Jakobs, G., 2007. Geology, McConnell Creek, British Columbia. Geological Survey of Canada Open File 5571; British Columbia Ministry of Energy, Mines and Petroleum Resources, Petroleum Geology Open File 2007-10, scale 1:125,000.

George, S.W.M., Nelson, J.L., Alberts, D., Greig, C.J., and Gehrels, G.E., 2021, Triassic–Jurassic accretionary history and tectonic origin of Stikinia from U-Pb geochronology and Lu-Hf isotope analysis, British Columbia: Tectonics, 40, paper e2020TC006505. https://doi.org/10.1029/2020TC006505

Gerstenberger, H., and Haase, G.A., 1997. Highly effective emitter substance for mass spectrometric Pb isotope ratio determinations. Chemical Geology, 136, 309-312.

Greig, C.J., Dudek, N.P., ver Hoeve, T.J., Newton, G., and Greig, R.E., 2021, Geology of the Tatogga property: Geologic framework for the Saddle North porphyry Cu-Au deposit and the Saddle South epithermal Au-Ag vein system, Iskut district, northwestern British Columbia. In: Geological Fieldwork 2020, British Columbia Ministry of Energy, Mines and Low Carbon Innovation, British Columbia Geological Survey Paper 2021-01, pp. 89-111.

Harriott, T.M., Crowley, J.L., Schmitz, M.D., Wartes, M.A., and Gillis, R.J., 2019, Exploring the law of detrital zircon: LA-ICP-MS and CA-TIMS geochronology of Jurassic forearc strata, Cook Inlet, Alaska, USA. Geology, 47, 1044-1048.

Hiess, J., Condon, D.J., McLean, N., and Noble, S.R., 2012. Systematics in terrestrial uranium-bearing minerals. Science, 335, 1610-1614.

Jaffey, A.H., Flynn, K.F., Glendenin, L.E., Bentley, W.C., and Essling, A.M., 1971. Precision measurements of half-lives and specific activities of 235U and 238U. Physical Review C, 4, 1889-1906.

Krogh, T.E., 1973. A low contamination method for hydrothermal decomposition of zircon and extraction of U and Pb for isotopic age determinations. Geochimica et Cosmochimica Acta, 37, 485-494.

Lord, C.S., 1948. McConnell Creek map-area, Cassiar District, British Columbia. Geological Survey of Canada Memoir 251, 82 p.

Mattinson, J.M., 2005. Zircon U-Pb chemical abrasion ("CA-TIMS") method: combined annealing and multi-step partial dissolution analysis for improved precision and accuracy of zircon ages. Chemical Geology, 220, 47-66.

Nasdala, L., Lengauer, C.L., Hanchar, J.M., Kronz, A., Wirth, R., Blanc, P., Kennedy, A.K., and Seydoux-Guillaume, A.M., 2002. Annealing radiation damage and the recovery of cathodoluminescence. Chemical Geology, 191, 121-140.

Nelson, J., Colpron, M., and Israel, S., 2013. The Cordillera of British Columbia, Yukon and Alaska: tectonics and metallogeny. In: Colpron, M., Bissig, T., Rusk, B., and Thompson, J.F.H., (Eds.), Tectonics, Metallogeny, and Discovery - the North American Cordillera and Similar Accretionary Settings. Society of Economic Geologists Special Publication 17, pp. 53-109.

Ootes, L., 2023. Did epithermal mineralization in the northern Toodoggone region develop synchronously with large-scale folding? In: Geological Fieldwork 2022, British Columbia Ministry of Energy, Mines and Low Carbon Innovation, British Columbia Geological Survey Paper 2023-01, pp. 13-21.

Ootes, L., Milidragovic, D., Friedman, R., Wall, C., Cordey, F., Luo, Y., Jones, G., Pearson, D.G., and Bergen, A., 2022. A juvenile Paleozoic ocean floor origin for eastern Stikinia, Canadian Cordillera. Geosphere, 18, 1297-1315. https://doi.org/10.1130/GES02459.1

Paton, C., Hellstrom, J., Paul, B., Woodhead, J., and Hergt, J. 2011. Iolite: Freeware for the visualisation and processing of mass spectrometric data. Journal of Analytical Atomic Spectrometry, 26, 2508-2518.

Schmitz, M.D., and Schoene, B., 2007. Derivation of isotope ratios, errors and error correlations for U-Pb geochronology using 205Pb-235U-(233U)-spiked isotope dilution thermal ionization mass spectrometric data. G3: Geochemistry, Geophysics, Geosystems, 8, paper Q08006. https://doi.org/10.1029/2006GC001492

Schmitz, M.D., and Davydov, V.I., 2012. Quantitative radiometric and biostratigraphic calibration of the global Pennsylvanian – Early Permian time scale. Geological Society of America Bulletin, 124, 549-577.

Vermeesch, P., 2018. IsoplotR: a free and open toolbox for geochronology. Geoscience Frontiers, 9, 1479-1493. https://doi.org/10.1016/j.gsf.2018.04.001

Vermeesch, P., 2021. Maximum depositional age estimation revisited. Geoscience Frontiers, 12, 843-850.

BRITISH COLUMBIA

Ministry of
Energy, Mines and
Low Carbon Innovation

BRITISH COLUMBIA
est. 1895
GEOLOGICAL SURVEY